

## Finger narrowing under local perturbations in the Saffman-Taylor problem

Giovanni Zocchi, Bruce E. Shaw, Albert Libchaber, and Leo P. Kadanoff

*The James Frank Institute, University of Chicago, 5640 South Ellis Avenue, Chicago, Illinois 60637*

(Received 8 April 1987)

We present an experimental study and a numerical simulation of the effect of time-independent, localized perturbations applied to the interface in the Saffman-Taylor fingering problem. When the perturbation is applied at a specific spot near the tip of the finger, the selection of the steady-state shape is drastically changed. In particular, one can obtain fingers with a width well below  $\lambda = \frac{1}{2}$ . A perturbation applied far away from the tip has no effect. We observe the same behavior in the simulation and in the experiment.

### INTRODUCTION

When air is pushed into a viscous fluid in a Hele-Shaw cell the steady-state shape of the interface is a finger whose width  $\lambda$  relative to the channel width depends on the dimensionless parameter  $B = \frac{1}{12}(b/W)^2 T/\mu V$  ( $b$  and  $W$  are the cell thickness and width,  $T$  is the surface tension,  $\mu$  the viscosity, and  $V$  the velocity of the steady finger). For zero surface tension ( $B=0$ ) and for symmetric fingers, Saffman and Taylor<sup>1</sup> found analytically a one-parameter family of solutions to the problem, with  $\lambda$  taking any value between 0 and 1. Allowing for asymmetric fingers, they found a two-parameter family of solutions, one parameter being the displacement of the finger from the center of the channel and the other being  $\lambda$ .<sup>2</sup> A finite surface tension has been shown to introduce a selection for the shape and restrict the number of solutions (for a given  $B$ ) to a discrete set, with only one of these solutions being stable and thus observable.<sup>3</sup> Experimentally obtained values of  $\lambda$  (from Ref. 4) are plotted in the upper curve of Fig. 1.

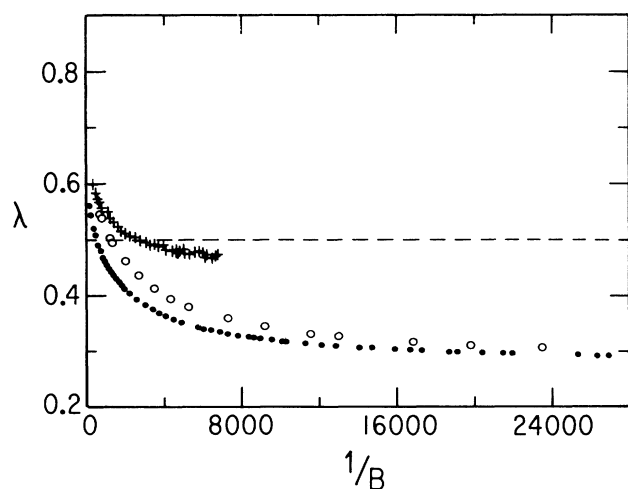


FIG. 1. Finger width  $\lambda$  vs  $1/B = 12(\mu V/T)(W/b)^2$ . +, unperturbed case (from Ref. 4);  $\circ$ , with a tungsten wire 13- $\mu\text{m}$  thick;  $\bullet$ , with a nylon wire 117- $\mu\text{m}$  thick.

It has been shown that experimentally it is possible to change the observed solutions by perturbing the interface. Grace and Harrison, in 1967, found narrowed solutions for rising bubbles in two and three dimensions when the bubble surrounded a rod that was placed in the channel.<sup>5</sup> Recently, Couder *et al.*<sup>6</sup> placed a small bubble at the tip of the finger and observed steady states with much smaller  $\lambda$ 's than in the unperturbed case. Hong and Langer have modeled these experiments by introducing a finite opening angle at the tip, and they find narrowed fingers.<sup>7</sup> Another way of obtaining narrow fingers is by introducing an anisotropy in the surface-tension parameter, that is by letting the surface tension vary along the interface. Under these circumstances, Kessler and Levine have found finger narrowing numerically and theoretically.<sup>8,9</sup> Dorsey and Martin have also obtained similar results.<sup>10</sup> In these studies, the length scale of the perturbation was of the order of the finger width.

Labeling and Libchaber<sup>4</sup> have observed asymptotic  $\lambda$  below  $\frac{1}{2}$  in experiments on "unperturbed" fingers. By introducing extra terms in the pressure drop at the interface to take into account three-dimensional film effects, Schwartz and DeGregoria,<sup>11</sup> and Sarkar and Jastrow<sup>12</sup> have numerically obtained similar results. By modifying the boundary conditions to allow for variable film thickness, Reinelt<sup>13</sup> has obtained good agreement with the experimental results.

Here we present an experimental study and a numerical simulation of the effects of local perturbations of the interface, i.e., perturbations whose length scale is much smaller than the finger width. In the experiment, a thin wire is suspended inside the channel parallel to the flow direction so that it intersects the interface, thereby creating a local deformation. In the numerical simulation, a local perturbation of the surface tension is introduced in the equations of motion. Despite the fact that the perturbation applied to the interface is quite different in the two cases, both the experiment and the simulation show the same qualitative and quantitative features of the resulting steady-state fingers: the selection of the solution is drastically changed (towards smaller values of  $\lambda$ ), when the perturbation is applied near the tip. The finger adjusts to put the perturbation in a specific place off centered from the tip. For a range of values of  $B$ , the dis-

tance of this particular spot from the tip scales as a power of the velocity, and we obtain, within the errors, the same scaling exponent from the experiment and the simulation. For this range of  $B$ , the tip curvature also scales as a power of the velocity, and again we find the same exponent in the simulation and in the experiment. However, at smaller values of  $B$  experimentally the finger width  $\lambda$  seems to approach an asymptotic value different from zero (due to numerical instabilities, we were not able to explore this region of  $B$  in the simulation). In the experiment we also find these thin fingers to be stable down to much smaller values of  $B$  than the unperturbed ones.

### EXPERIMENTAL OBSERVATIONS

The Hele-Shaw cell and the fluids used in the experiment (air against oil) were the same as in Ref. 4. The cell had dimensions  $W=5$  cm,  $b=0.8$  mm, and the parameters of the oil were  $\mu=5$ ,  $T=23$  in cgs units. The perturbation applied to the interface consisted in suspending a thin wire inside the cell. The wire was parallel to the flow direction and extended along the complete length of the cell. It was kept in place (at midheight of the channel gap) by supports at both ends of the cell, and it was put under tension by attaching weights to its ends. Different types of wire were used in the experiments: a  $117\text{-}\mu\text{m}$  thick nylon wire, and  $100\text{-}\mu\text{m}$  and  $13\text{-}\mu\text{m}$ -thick tungsten wires.

If the wire does not touch the interface, the perturbation of the flow it causes seems irrelevant to the interface dynamics, that is, one obtains a "normal" finger [Fig. 2(a)]. If the wire does intersect the interface then the constraint of the contact angle at the wire-oil-air interface produces a local deformation of the latter. Two different states are possible, depending on whether the wire intersects the finger near the tip or far away from it. In Fig. 2(b) the wire has been shifted a little towards the center of the channel, as compared to Fig. 2(a), so that it intersects the interface far away from the tip. We see that apart from a local deformation the overall shape is the same as in Fig. 2(a); in particular the width  $\lambda$  is the same (in the two figures the velocity of the finger is nearly the same). In Fig. 2(c) the wire has been shifted still more towards the center, and now we see that the whole finger adjusts itself laterally in the channel to put the wire in a specific position near the tip. In this "perturbed" state the value of  $\lambda$  is drastically different from the unperturbed case; for example, the finger in Fig. 2(c) is considerably thinner than in the two previous pictures, even though the velocity is actually smaller in Fig. 2(c). For small values of  $B$  the shapes of these thin fingers is, apart from the small bump caused by the wire, indistinguishable from the Saffman-Taylor (zero surface tension) solution with the same width  $\lambda$ .

Figure 2(d) shows that even when the wire is displaced away from the center of the channel, with proper initial conditions one can still obtain a thin finger which is "guided" by the wire [in this figure the wire is in the same position in the channel as in Fig. 2(b)]. The shape is here asymmetric because the finger is not moving in

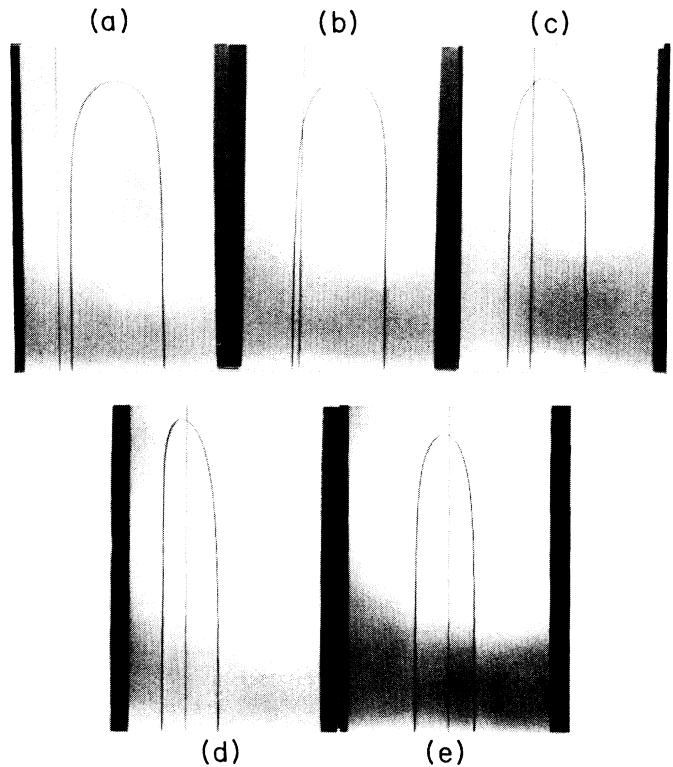


FIG. 2. Steady-state fingers of air penetrating into oil. (a)–(d) A nylon wire with a diameter of  $117\text{-}\mu\text{m}$  is suspended inside the cell; (e) a  $13\text{-}\mu\text{m}$  thick tungsten wire is used. (The wires have been retouched on the figure.) (a)  $1/B=3160$ ,  $\lambda=0.482$ ; the wire does not intersect the interface, and there is no effect on the shape. (b)  $1/B=3000$ ,  $\lambda=0.481$ ; the wire intersects the interface far away from the tip, and still there is no effect on the overall shape. (c)  $1/B=2510$ ,  $\lambda=0.402$ ; the wire intersects the interface near the tip, and the finger width is dramatically changed. (d)  $1/B=17\,200$ ,  $\lambda=0.296$ . The shape is asymmetric because the finger is not moving in the middle of the channel. (e)  $1/B=28\,300$ ,  $\lambda=0.300$ .

the middle of the channel. For small  $B$  this shape is again indistinguishable from the zero surface-tension solution for a finger propagating asymmetrically in the channel.<sup>2</sup>

Thus we observe that if a localized perturbation (in this case the deformation of the interface caused by the wire) is applied far away from the tip, then it has no effect on the finger width, while if it is applied at a specific spot near the tip, then it changes the finger width dramatically: for a given  $B$  one obtains a much thinner finger than the corresponding unperturbed one; in particular, one obtains finger widths well below  $\lambda=\frac{1}{2}$  (Fig. 1). This qualitative behavior does not seem to depend on the details of the perturbation applied to the interface. Figure 1 shows that two wires with radii differing by an order of magnitude produce qualitatively the same effect.

In these perturbed states the wire is in a specific position with respect to the tip, and this position depends on

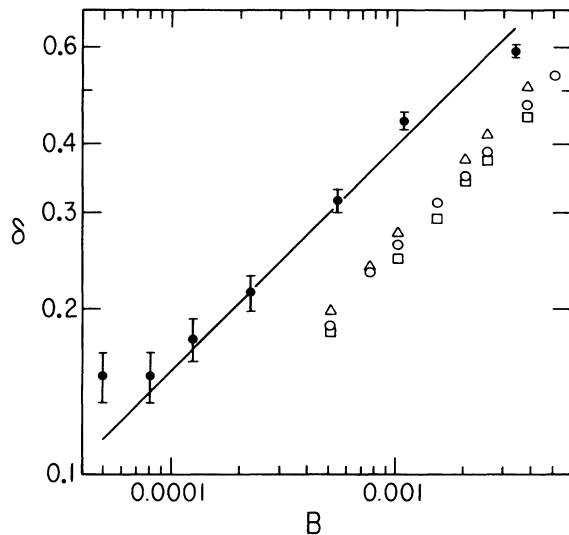


FIG. 3. Log-log plot of  $\delta$ , the distance from the tip to the wire, vs  $B$ ;  $\delta$  is in units of  $W/2\pi$ ; the straight line has a slope of 0.4. The top curve is the experimental data, obtained using a  $117\text{-}\mu\text{m}$  nylon wire. The three lower curves are the results from the simulation for three different values of the perturbation amplitude  $A$ . (Here  $A$  measures the amplitude of the perturbation, with the surface tension increasing by a factor of  $1+A$  at the center of the disturbance.) The curves for the simulation are denoted by the following:  $\triangle$ ,  $A=0.5$ ;  $\circ$ ,  $A=2$ ;  $\square$ ,  $A=4$ .

the velocity. For  $B$  between 0.0001 and 0.003 we find the distance  $\delta$  between the tip and the wire to scale as  $\delta \sim V^{-\alpha}$  with  $\alpha=0.40 \pm 0.04$  (Fig. 3).

The second striking result concerns the stability of these thin fingers: they are found to be stable in a much larger range of the control parameter than the unperturbed ones. In Fig. 1 the curve corresponding to the unperturbed ( $\lambda \sim \frac{1}{2}$ ) fingers is plotted up to a value of the parameter  $1/B$  of about 7000, which is, for the noise level characteristic of this experimental setup, the threshold for the onset of instabilities<sup>4</sup>; the thin fingers obtained with the wires (in the same cell, and thus with at least the same level of noise) are instead stable up to much higher values of  $1/B$ : The first instabilities appear for  $1/B \sim 80\,000$ , i.e., more than ten times the threshold for the unperturbed case. Figure 2(e) shows a thin finger with  $1/B=28\,300$ . (This increased stability was also noted by Grace and Harrison<sup>5</sup>.)

In view of possible future theoretical work, the question arose as to the possibility of obtaining thin steady-state fingers applying a symmetric perturbation to the interface. We thus introduced two parallel wires in the channel, a distance  $D$  apart from each other. The resulting behavior is shown in Fig. 4: For a given spacing  $D$ , at low enough velocities one obtains a symmetric steady state for which the selection is indeed different from the unperturbed case; as the velocity is increased, a transition to an asymmetric state occurs [Fig. 4(b)], in which the tip "chooses" one of the wires. In the asymmetric

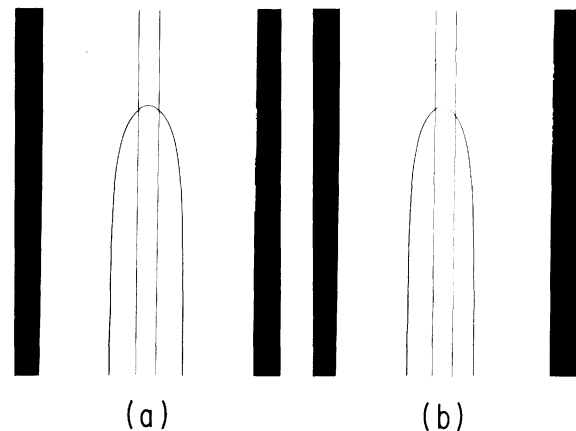


FIG. 4. Fingers in a cell with two parallel  $100\text{-}\mu\text{m}$  thick tungsten wires a distance  $D=4.72$  mm apart. (a)  $1/B=6110$ ,  $\lambda=0.345$ ; symmetric state. (b)  $1/B=21\,600$ ,  $\lambda=0.315$ ; asymmetric state. (The wires have been retouched on the figures.)

state the selection is determined by the wire nearest to the tip, and the second wire has no effect; this is shown in Fig. 5, where we plot, for two different wire spacings, the values of  $\lambda$  before and after the transitions from the symmetric to the asymmetric state. For comparison, the curve obtained with only one wire (asymmetric state) is also plotted. We see that all the asymmetric states coincide.

#### SIMULATION OF PERTURBED INTERFACE

In the simulation, we tried to reproduce the phenomena seen in the experiments. It was found that by varying

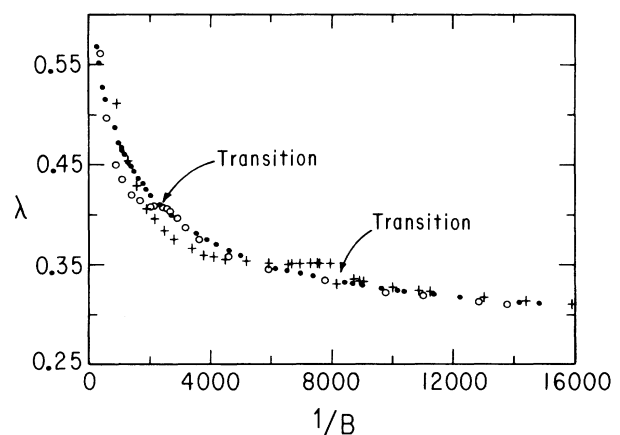


FIG. 5. Finger width  $\lambda$  vs  $1/B$  for a cell with two parallel  $100\text{-}\mu\text{m}$  thick tungsten wires.  $\circ$ , the distance between the wires is  $D=6.64$  mm; the shape is symmetric for  $1/B < 2000$  and asymmetric thereafter; the transition is marked.  $+$ , same as above with  $D=4.72$  mm; now the transition symmetric-asymmetric state occurs for  $1/B \sim 8000$ .  $\bullet$ , data obtained with one  $117\text{-}\mu\text{m}$  thick nylon wire (asymmetric state).

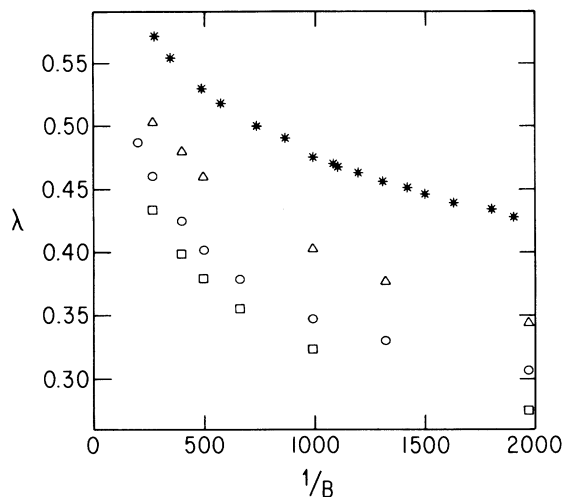


FIG. 6. Width of the finger  $\lambda$  vs  $1/B$  for three different amplitudes of the perturbation, and the experimental data for the 117- $\mu\text{m}$  nylon wire for this range. The experimental curve is denoted by \*, and the curves for the simulation are denoted by the following:  $\Delta$ ,  $A = 0.5$ ;  $\circ$ ,  $A = 2$ ;  $\square$ ,  $A = 4$ .

the surface tension parameter in a local region which could move along the interface, we indeed saw most of the essential features observed experimentally. The widths of the fingers were significantly reduced, with  $\lambda$  much below  $\frac{1}{2}$  seen (Fig. 6). A perturbation which increased the surface tension produced different results depending upon where it was initially placed. Placements far from the tip had essentially no effect. Ones beginning near the tip would move with respect to the finger until they were a specific distance away from the tip; then, a new narrower finger width would be chosen. The above results apply when the region in which the surface tension varies is very small compared to the fingerwidth. In this way we mimicked the experiments with a single wire. When we put in two regions of nonconstant surface tension to mimic the two wires experiment, the simulation produced a symmetric finger when the regions were close to one another and an asymmetric one when they were further apart.

#### DESCRIPTION OF THE SIMULATION

David Bensimon<sup>15</sup> developed a simulation to study the growth of fingers in Hele-Shaw cells. We have taken his program and modified it to allow for local changes in the surface tension parameter. The simulation calculates the time evolution of a set of points representing the interface between two fluids. The points move with a normal velocity proportional to the normal gradient of the pressure field, and with a tangential velocity along the interface which is chosen to keep the mapping analytic. (See Ref. 15 and a review article by Bensimon, *et al.*<sup>16</sup> for a discussion of the technique used and a derivation of the equations of motion.) We perturbed the interface by associating with each point a fixed specific surface tension; it is uniform in the case of an unperturbed surface, but

varying in the perturbed one.

Specifically, we choose the surface tension at the  $s$ th point on the interface to have the form  $T(s) = T_0(1 + Ae^{-(s-s_0)^2/D^2N^2})$ . Here  $A$  is the amplitude of the perturbation,  $D$  its width,  $N$  the number of points on the interface, and  $s_0$  is the center of the disturbance. The “points” on the interface are, of course, just a theoretical artifice. In the real experiment the perturbation is not tied to any set of points but instead has a fixed position in real space. The way the perturbation enters into the boundary conditions of the interface are thus quite different. The wire in the experiment determines the shape of the interface locally through the fixing of the contact angle, while in the simulation the shape of the perturbation is found along with the interface by way of a free boundary problem. Further, the nonphysical velocities with which the points move to keep the mapping analytic also add additional time dependence to the perturbation. The connection between the dynamics of the simulation and the experiment is thus not at all clear. However, once a steady state is reached the simulation and the experiment may be directly compared.

We used the point-based perturbation because it was computationally convenient. For further convenience, we chose to represent the side walls by using periodic boundary conditions. These require that the velocity field be repetitive under a lateral displacement by a cell width. This corresponds to a geometry of closely spaced concentric cylinders. A better boundary condition for the plane rectangular geometry would be to require the normal component of the velocity to vanish at the cell walls.

The limitations of the simulation came from numerical instabilities, which constrained the ranges of  $B$  we were able to explore to roughly a decade from  $5 \times 10^{-4} < B < 5 \times 10^{-3}$ . Also, constraints on smoothness limited the narrowness of our perturbations. The program was run in vectorized FORTRAN on an Floating Point Systems FPS364 array processor. Typical runs took 15 000 iterations to reach a steady state, with run times of 5000 iterations/h for 512 points.

#### STEADY STATES OF THE INTERFACE

There were only a few specific places where the perturbation would end up in the steady state. For example, for amplitudes  $A < 0$ , there was only one stable fixed point. These local reductions in surface tension drifted to the tip. Then steady states with  $\lambda$  greatly reduced would be reached (including  $\lambda$  much below  $\frac{1}{2}$ ). The unique steady state for  $A < 0$  contrasted with the case of  $A > 0$ , which had different final states depending on where the perturbation was initially placed; we saw several (usually two or three) “basins of attraction” on each side of the finger. If the initial perturbation was placed far enough back then it would drift toward the base of the finger and have no effect. However, a placement near but not at the tip would produce a drift to a well-defined point, as in Fig. 7. This “fixed point” is the eventual destination of all perturbations initially in a

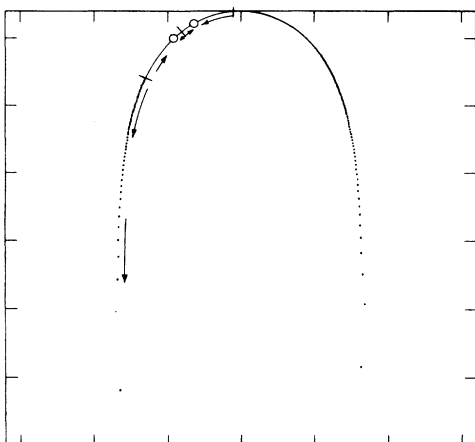


FIG. 7. Basins for increased surface-tension perturbations along finger interface. The same perturbation starting anywhere within a basin will produce the same steady state, with the perturbation located at the fixed point (denoted by "o") for that basin. Perturbations starting far from the tip drift back. Perturbations starting near the tip move to the forward fixed point. Depending on the ranges of the parameters, the middle basin may or may not exist. When it does, the fingers reach a steady state with the perturbation at the fixed point shown; when it does not, this basin merges with the one in front and the forward fixed point becomes the final position for perturbations beginning in the combined regions.

basin near the tip. For some ranges of the parameters—larger values of  $B$  and small enough amplitudes in the perturbation—an additional basin between the two just discussed was seen (Fig. 7). The largest reductions in  $\lambda$  compared with the unperturbed case arose from the fixed point nearest to the tip (Fig. 8).<sup>17</sup> Using this fixed point, we obtained scaling laws for the steady-state solutions. For the range of parameters of the perturbation studied, and for  $B$  between  $5 \times 10^{-4}$  and  $5 \times 10^{-3}$ , the tip curvature varies as  $\kappa_{\text{tip}} \sim B^{-0.49 \pm 0.02}$  (Fig. 9). In the unperturbed case, the scaling is  $\kappa_{\text{tip}} \sim B^{-0.16 \pm 0.02}$  for this range of  $B$  (Fig. 9). Notice that if the finger width reaches an asymptotic limit different from zero, as is suggested by the experiments, then these scalings cannot represent an asymptotic limit, but are to be taken only as a fit for this range of  $B$ . While the tip curvature was not measured experimentally, if we assume the shape to be close to a Saffman-Taylor solution, we can get a value for  $\kappa_{\text{tip}}$  from  $\lambda$ . In this intermediate range for  $B$ , this analysis of the experimental data gives the scaling  $\kappa_{\text{tip}} \sim B^{-0.46 \pm 0.02}$  (Fig. 9). A second quantity we can measure is the displacement  $\delta$  of the perturbation from the tip. For this range in  $B$  we find in the simulation that  $\delta$  scales as  $\delta \sim B^{0.45 \pm 0.02}$  (Fig. 3); this compares to the exponent  $0.40 \pm 0.04$  obtained in the experiments. The quoted errors are numerical uncertainties; systematic errors are unknown.

Another phenomenon observed experimentally was also reproduced in the simulation. In the experiments,

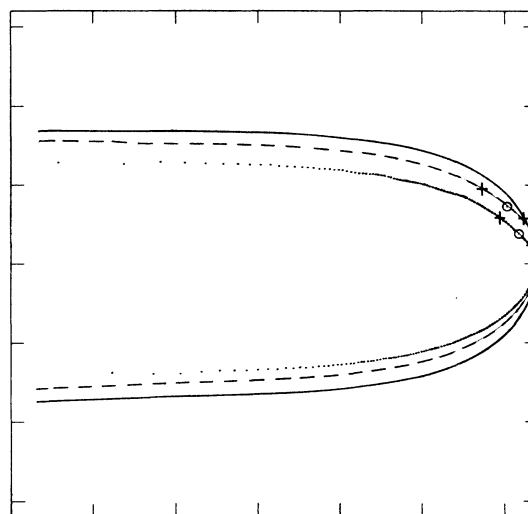


FIG. 8. Three different steady-state fingers obtained with the same value of  $B$ , the same perturbation, and different initial locations of the perturbations. The finger for the back basin, shown by the solid line, is indistinguishable from the unperturbed case. For the other two fingers, the circle  $\circ$  marks the location of the perturbation peak, and the extent of it, defined by the amplitude falling to less than 1% of the peak, is marked by the + on each side. The perturbation is a local increase of the ambient  $B = 2.5 \times 10^{-3}$  with an amplitude  $A = 2$ . The dashed line is for the basin in the middle. The dotted finger is for the basin closest to the tip (these dots are what is actually seen in the simulation; the lines above are an interpolation between the points).  $\lambda$  for the three fingers shown are 0.44, 0.50, and 0.55.

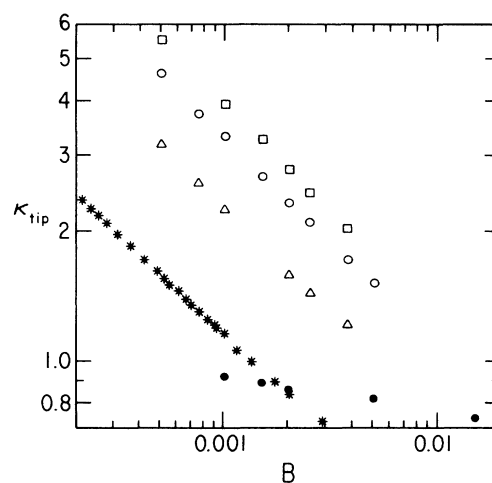


FIG. 9. Log-log plot of the tip curvature  $\kappa_{\text{tip}}$  vs  $B$ . The three upper curves are from the simulation with three strengths of the perturbation.  $\square$ ,  $A = 4$ ;  $\circ$ ,  $A = 2$ ;  $\triangle$ ,  $A = 0.5$ . The experimental curve is marked by  $*$ . The unperturbed simulation, where  $A = 0$ , is marked by the solid circle  $\bullet$ .

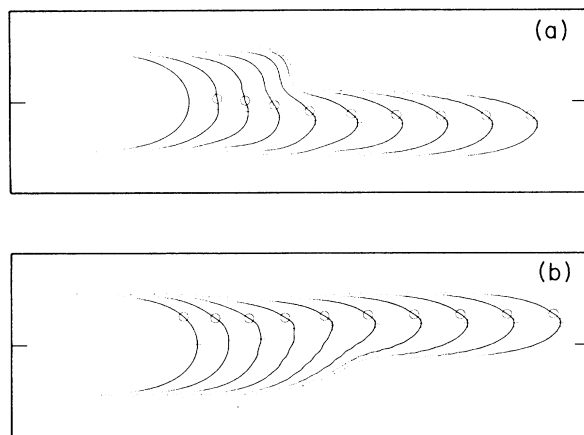


FIG. 10. Two evolving fingers with increased surface tension perturbation, showing the transition to the new  $\lambda$  once the perturbation reaches the fixed point. The cross marks the tip, while the circle shows the location of the peak of the perturbation. The difference between the two fingers is where the perturbation is initially placed. In (a) the perturbation starts closer to the tip than the fixed point, while in (b) it starts behind the fixed point. In both cases the long-term steady state will be the same.

there was a transition from a symmetric to an asymmetric state when the spacing between two wires was increased. To represent a situation in which there were two separated regions of perturbation, we used a surface tension which had three flat regions

$$T(s) = \begin{cases} T_0 & \text{for } s < s_0 \\ T_0(1+A) & \text{for } s_0 < s < s_1 \\ T_0 & \text{for } s > s_1 \end{cases},$$

and then varied smoothly at the junction between these regions. We studied the evolution of a finger in which this perturbation was applied initially in a slightly asymmetrical position. For small widths of the perturbation, it drifted to a symmetric position with respect to the tip. However, as the width was increased above a certain amount, the perturbation drifted to a position

asymmetrical with respect to the tip, with one of the transition regions between the steps of the perturbation hanging out in a preferred spot.

The dynamics of the selection of the perturbed solution was also quite interesting. While the perturbation was drifting to the preferred position on the interface, the finger remained relatively unaffected, even for perturbations closer to the tip than the preferred spot. Once the perturbation came close to its final position, the finger shape changed markedly. A narrower front of the finger was formed, and this grew out of the old fatter one (Fig. 10).

## CONCLUSION

We present some new phenomenology on the effects of perturbing the interface in the Saffman-Taylor problem. The selection of the shape is modified by a localized, time-independent perturbation. The perturbation has an effect only if it is applied near the tip. The change in selection always results in  $\lambda$  being decreased. We have been able to reproduce the phenomena seen with a complicated experimental perturbation—involving three-dimensional effects and nonsmooth kinks in the interface—in a simulation using smooth local variations in the surface-tension parameter. This reformulation of the problem should lend itself to analytical studies. In the experiment, for very small values of  $B$ , an asymptotic state with a nonzero value of  $\lambda$  appears to be approached. We also observe a transition from a symmetric to an asymmetric solution when the separation between two disturbances (two wires in the experiment, two gradients in the surface-tension parameter in the simulation) is increased above a certain amount. Experimentally, we also find the thin fingers to be stable down to much smaller values of  $B$  than the unperturbed ones.

## ACKNOWLEDGMENTS

We would like to thank David Bensimon for the use of his program. This work was supported by the National Science Foundation (NSF) under Grant No. DMR-83-16626 and by the University of Chicago Materials Research Laboratory.

<sup>1</sup>P. G. Saffman and G. I. Taylor, Proc. R. Soc. London, Ser. A **245**, 312 (1958).

<sup>2</sup>G. I. Taylor and P. G. Saffman, Q. J. Mech. Appl. Math. **12**, 265 (1959).

<sup>3</sup>For a review of the field, and current understandings and questions, see P. G. Saffman, J. Fluid Mech. **173**, 73 (1986). For papers on selection and stability due to surface tension, see these and references contained within J. W. McLean and P. G. Saffman, J. Fluid Mech. **102**, 445 (1981); J. M. Vanden-Broeck, Phys. Fluids **26**, 2033 (1983); D. A. Kessler and H. Levine (unpublished); and Phys. Rev. Lett. **57**, 3069 (1986); D. Bensimon, P. Pelce, and B. Shraiman (unpublished); S. Tanveer (unpublished).

<sup>4</sup>P. Tabeling, G. Zocchi, and A. Libchaber, J. Fluid Mech. **177**, 67 (1987).

<sup>5</sup>J. R. Grace and D. Harrison, Chem. Eng. Sci. **22**, 1337 (1967).

<sup>6</sup>Y. Couder, N. Gerard, and M. Rabaud, Phys. Rev. A **34**, 5175 (1986).

<sup>7</sup>D. C. Hong and J. S. Langer, Phys. Rev. Lett. **56**, 2032 (1986).

<sup>8</sup>D. A. Kessler, J. Koplik, and H. Levine, Phys. Rev. A **34**, 4980 (1986).

<sup>9</sup>D. A. Kessler and L. Sander, Phys. Rev. A **34**, 4 (1986); **34**, 3535 (1986). Figure 1 shows finger narrowing under a long-wavelength surface-tension perturbation.

<sup>10</sup>A. T. Dorsey and O. Martin, Phys. Rev. A **35**, 3989 (1987).

<sup>11</sup>L. W. Schwartz and A. J. DeGregoria, Phys. Rev. A **35**, 276 (1986).

<sup>12</sup>S. Sarkar and D. Jastrow (unpublished).

<sup>13</sup>D. A. Reinelt (unpublished).

<sup>14</sup>In an experiment currently in progress we study the behavior

of the finger under perturbations localized both in time and space. We achieve this by switching a high voltage on and off the wire. We observe that the wavelength characteristic of the response of the system to these perturbations also scales as a power of the velocity with this same exponent  $\alpha=0.4$ .

<sup>15</sup>D. Bensimon, Phys. Rev. A **33**, 1302 (1986).

<sup>16</sup>D. Bensimon, L. P. Kadanoff, S. Liang, B. I. Shraiman, and C. Tang, Rev. Mod. Phys. **58**, 977 (1986).

<sup>17</sup>Some oscillatory motion behind the perturbation was sometimes seen in the strongly perturbed increased surface tension "steady states," as can be seen in the tail of the forward basin solution of Fig. 8.

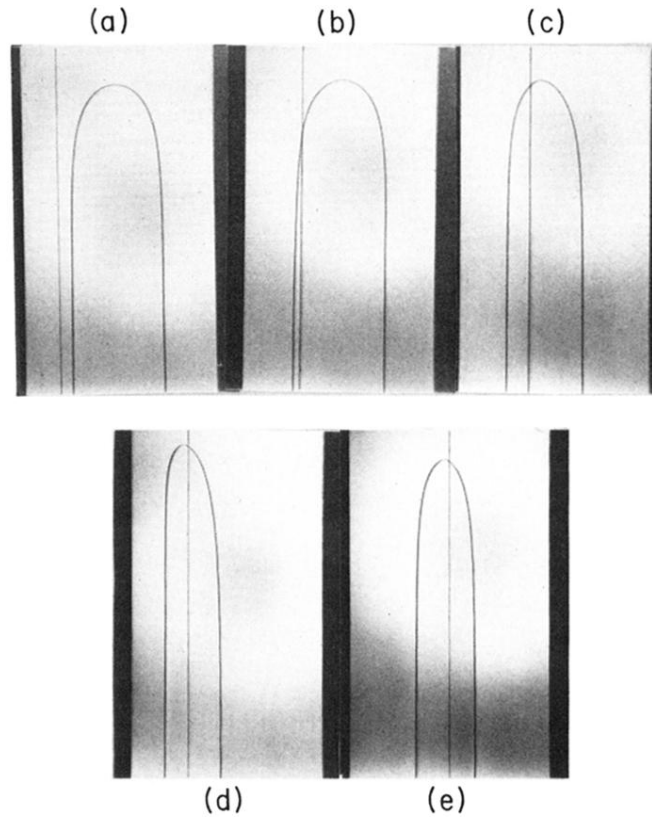


FIG. 2. Steady-state fingers of air penetrating into oil. (a)–(d) A nylon wire with a diameter of  $117\text{-}\mu\text{m}$  is suspended inside the cell; (e) a  $13\text{-}\mu\text{m}$  thick tungsten wire is used. (The wires have been retouched on the figure.) (a)  $1/B = 3160$ ,  $\lambda = 0.482$ ; the wire does not intersect the interface, and there is no effect on the shape. (b)  $1/B = 3000$ ,  $\lambda = 0.481$ ; the wire intersects the interface far away from the tip, and still there is no effect on the overall shape. (c)  $1/B = 2510$ ,  $\lambda = 0.402$ ; the wire intersects the interface near the tip, and the finger width is dramatically changed. (d)  $1/B = 17\,200$ ,  $\lambda = 0.296$ . The shape is asymmetric because the finger is not moving in the middle of the channel. (e)  $1/B = 28\,300$ ,  $\lambda = 0.300$ .